



Experimental and numerical investigation of residual stresses in proximity girth welds

Sachin Bhardwaj¹ · Sigmund Kyrre Aas² · R. M. Chandima Ratnayake¹ 

Received: 20 October 2022 / Accepted: 23 February 2023 / Published online: 9 March 2023
© The Author(s) 2023

Abstract

International fabrication codes and standards provide minimum distance criteria for proximity welds, although rigorous justification is lacking. These distances are either based on practical experience or mutual agreement and are often left to the engineering judgment of contractors, inspection engineers, etc., especially in cases of repair welds fabricated in proximity to existing welds. Previous studies have shown high tensile residual stresses and altered mechanical and microstructural properties between proximity welds. This article focuses on numerical and experimental quantification of residual stresses in the proximity region by X-ray diffraction (XRD) and finite element method (FEM) thermo-mechanical models. Specimens were machine welded, then repair welded at distances of 5–15 mm. A fair agreement in results was achieved between FEM and XRD. The most detrimental effect was observed at the weld root toe for the repair weld at 5 mm proximity, likely due to the high constraint and multiaxial stress state. These findings enable practitioners to propose technical justification and corrective actions while specifying minimum distance criteria for proximity welds.

Keywords Residual stresses · Thermo-mechanical · Proximity repair welds · X-ray

1 Introduction

Pipe replacement procedures are inevitable in high-pressure piping structures. The causes vary and include high temperature creep effects, development of tensile residual stresses at weld toes, intersection of longitudinal welds with girth welds, internal corrosion, and overlap of reinforcement of branch connections with existing welds [1]. These situations lead to the fabrication of repair welds in proximity to existing welds like welds of branch connections, nozzles, etc., during pipe replacement procedures. Failures due to repair weld proximity to existing welds have led to catastrophic incidents in structural offshore brace joints [2], nuclear power piping girth welds [3], and offshore floating structural members [4] due to the development of deleterious

tensile residual stresses at weld toe locations. International fabrication and repair codes lack clear consensus when it comes to deciding the minimum distance between welds as described in a previous review [5]. These fabrication codes lack consensus for deciding minimum proximity distance criteria, which is recommended either based on the thickness factor (four to five times) or diameter (one to one and a half times) of the joining member. Repair procedures of fabrication codes are purely based on mutual agreement or some set arbitrary distance that is based on the operator's practical experience as stated in API 2200 [6] and DNV-OSF101 [7], which are used in transportation pipelines and subsea pipe replacement guides, respectively.

Repair welds are widely used in replacement procedures to extend aging piping's life [8], which are often vulnerable to cracking due to stress corrosion cracking (SCC) at the weld root or at a distance away from weld toe locations. Tensile residual stress coupled with corrosive medium in pipe internal surfaces represents a risk for SCC cracking at weld root locations [1]. Repair welds can develop further restraint in addition to the original restraint of girth welds, which can further develop harmful or beneficial residual stresses across the thickness of proximity regions [8, 9]. Increases in transverse residual stresses (perpendicular to the weld) have

✉ R. M. Chandima Ratnayake
chandima.ratnayake@uis.no

¹ Department of Mechanical and Structural Engineering and Materials Science, University of Stavanger, N-4036 Stavanger, Norway

² Department of Marine Technology, Faculty of Engineering, Norwegian University of Science and Technology (NTNU), NO-7491 Trondheim, Norway

been observed by various researchers [3, 8–10] in repair regions of existing welds, which are important from a structural integrity perspective. Proximity regions that develop between repair and existing welds are subjected to multi-axial stress states due to the presence of additional restraints, which can increase the through-thickness membrane and bending component as per stress decomposition theory [9]. Level 3 assessment of estimating welding-induced residual stresses (WRS) in structural integrity procedures of fitness for service codes [11–13] requires the use of nonlinear FEM results coupled with residual stress experimental measurements for defining residual stress profiles at a distance away from weld toe locations, which are currently practically non-existent or overly conservative [14, 15].

Changes in transverse residual stress profiles have been observed between offshore jacket brace joints and proximity butt welds in plates fabricated with a similar welding process in the past [16, 17]. Weld sequence and additional restraint due to the heat input of additional welds play important roles in estimating final WRS profiles [18]. We previously qualified the welding procedure between repair and existing girth welds [4] by welding with two different welding processes where high hardness and low Charpy energy values were recorded. Further development of high tensile axial residual stresses at mid thickness and towards the root region of proximity welds was observed between repair and existing welds by using the neutron diffraction (ND) technique [19]. There is a lack of studies on the distribution of WRS around weld root and toe locations to estimate stresses on pipe outer and inner surfaces.

This study aimed to investigate how repair girth weld placement at set distances of 5, 10, and 15 mm from the existing weld impacts the residual stress distribution around weld toe and root regions. The thermo-mechanical-based finite element method (FEM) using ABAQUS was used to simulate the welding process and estimate residual stresses. Experimental validation was performed by using X-ray diffraction (XRD) to evaluate residual stresses at the pipe outer and inner surfaces. The remainder of the paper is structured

as follows: Section 2 presents the methodology. In Section 3, the results are presented and discussed. Finally, in Section 4, we draw our conclusions.

2 Methodology

2.1 Test specimens

Proximity girth welds were fabricated on structural steel grade S355 G14 + N seamless pipe, with dimensions of 219.1 mm outside diameter and 8.18 mm thickness. To simulate the practical scenario of proximity welds, an initial weld (A) was welded with the tungsten inert gas (TIG) welding process. After maintaining the required weld proximity (WP) distance of 5, 10, or 15 mm between adjacent weld toes, a repair weld (B) was fabricated with metal active gas (MAG) for the root pass, and Flux-cored arc welding (FCAW) was used for the remaining passes. Details for the welding parameters and mechanical properties of the base and filler wire can be found in our previous work and briefly summarized in Table 1 [4].

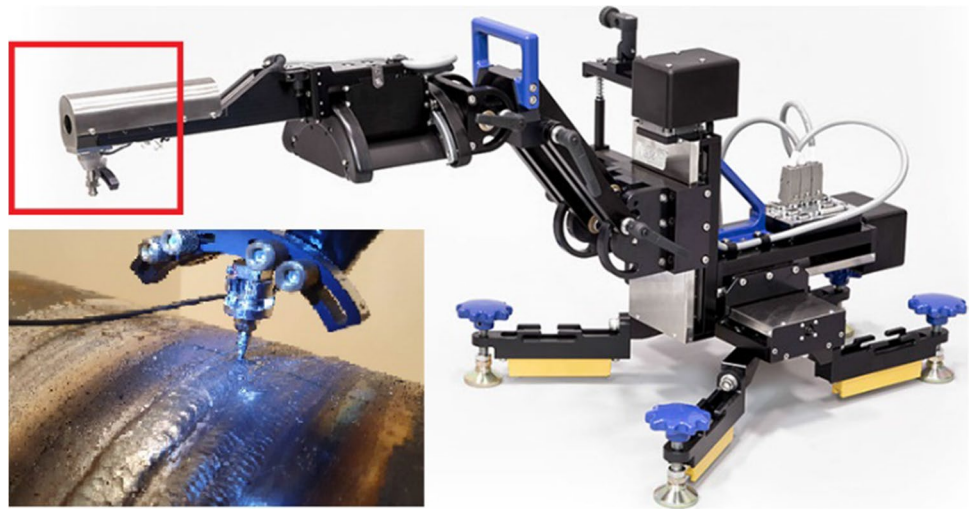
2.2 Residual stress measurements using X-ray diffraction

WRS was measured using a Proto iXRD instrument on the inner and outer surfaces of the welded pipes as shown in Fig. 1 Stress calculations are done in Proto XRDWIN using the $\sin^2 \Psi$ method and 11 β angles. A β range of $\pm 20^\circ$ was used for the outside of the pipe, while the inside was restricted to $\pm 16^\circ$ due to collision with the pipe wall. A Cr cathode was used with a 1 mm circular aperture at 20 kV and 4 mA, which gives a penetration depth of about 4–5 μm [20]. Measurement locations were manually chosen as close to the roots as was feasible and at 3–5 mm intervals. The locations were programmed so that subsequent measurements could be obtained at the exact same points in both the axial and

Table 1 Welding parameters for weld A, TIG welding process and welding parameters for weld B, MAG + FCAW welding process

Pass	Weld	Filler (mm)	Welding process	Current (A)	Voltage (V)	Polarity	Travel speed (mm/min)	Gas flow (l/min)	Heat input (kJ/mm)
1	A	2.4	TIG	100–135	10–20	DC-	39–40	15–20	1.5–2.49
2	A	2.4	TIG	140–180	10–14	DC-	75–80	15–20	1.05–2.02
Fill	A	2.4	TIG	160–230	11–15	DC-	85–120	15–20	0.88–2.44
Cap	A	2.4	TIG	160–230	11–15	DC-	85–120	15–20	0.88–2.44
1	B	1.2	MAG	90–125	14–16	DC+	65–85	16–20	0.89–1.85
2	B	1.2	FCAW	160–220	22–29	DC+	180–400	16–20	0.53–2.13
Fill	B	1.2	FCAW	180–250	22–29	DC+	180–400	16–20	0.59–2.42
Cap	B	1.2	FCAW	180–250	22–29	DC+	180–400	16–20	0.59–2.42

Fig. 1 Proto iXRD instrument measuring residual stresses on pipe outer surface [21]



hoop directions. All measurements were taken at the surface level of the pipe on the inner and outer surfaces, respectively.

2.3 Numerical model

In this study, a FEM-based numerical model was generated in ABAQUS [21] using the Qustom app plugin [22] which was used to develop automatic subroutines for multi-pass welds. In thermo-mechanical-based FEM models, temperature history output serves as input to mechanical models. Nodal temperature distribution is solved incrementally in mechanical models with time to satisfy equilibrium conditions [23]. It is important to mention here that an uncoupled thermo-mechanical simulation was used in this analysis, which generates separate thermal and mechanical models. Mechanical strains are estimated according to simulated heating and cooling times from a temperature distribution of existing and repair welds, which replicates the practical pipe replacement procedures. However, the effects of initial residual stresses were taken as negligible as reported by past research [8, 9]. Hence, WRS was measured after the completion of the repair weld only.

2.3.1 Geometry

A 2D Axisymmetric model was built in ABAQUS from available macrographs of existing and repair welds. Three different scenarios of WP distances of 5, 10, and 15 mm were maintained between adjacent weld toes as shown in Fig. 2 with a minimum element size of 0.15 mm maintained at HAZ and proximity regions. A mesh convergence study was performed and was found to be satisfactory as the residual stresses profile did not change with increasing element size. Subsequently, repair welds were modeled according to an available macrograph from the welding qualification procedure record (WPQR) [4] at set proximity distances. Existing and repair welds were modeled simultaneously; however, during thermal analysis, repair weld was made inactive using the “model change” feature in ABAQUS to develop automatic subroutines by use of the Qustom app plugin.

2.3.2 Material model

Temperature-dependent material and mechanical, material and hardening properties for the parent and weld metals were taken from Bhatti et al. [24] as also shown in Fig. 3a

Fig. 2 Axisymmetric FEM model of existing and repair welds reproduced from weld macrographs showing XRD measurement locations

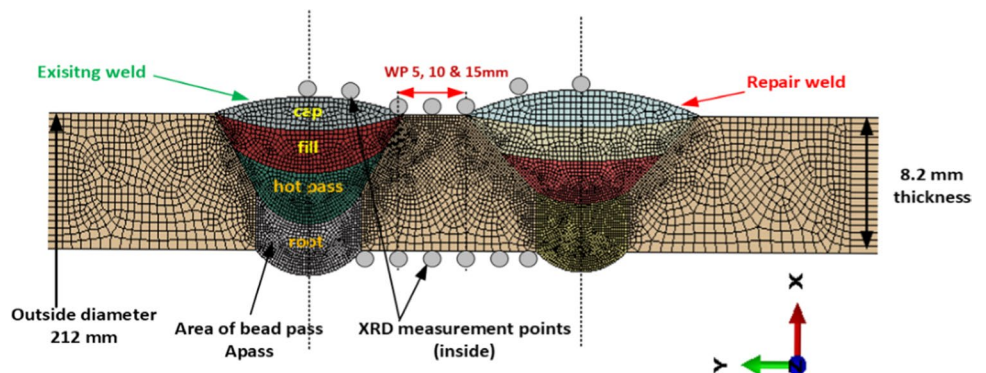
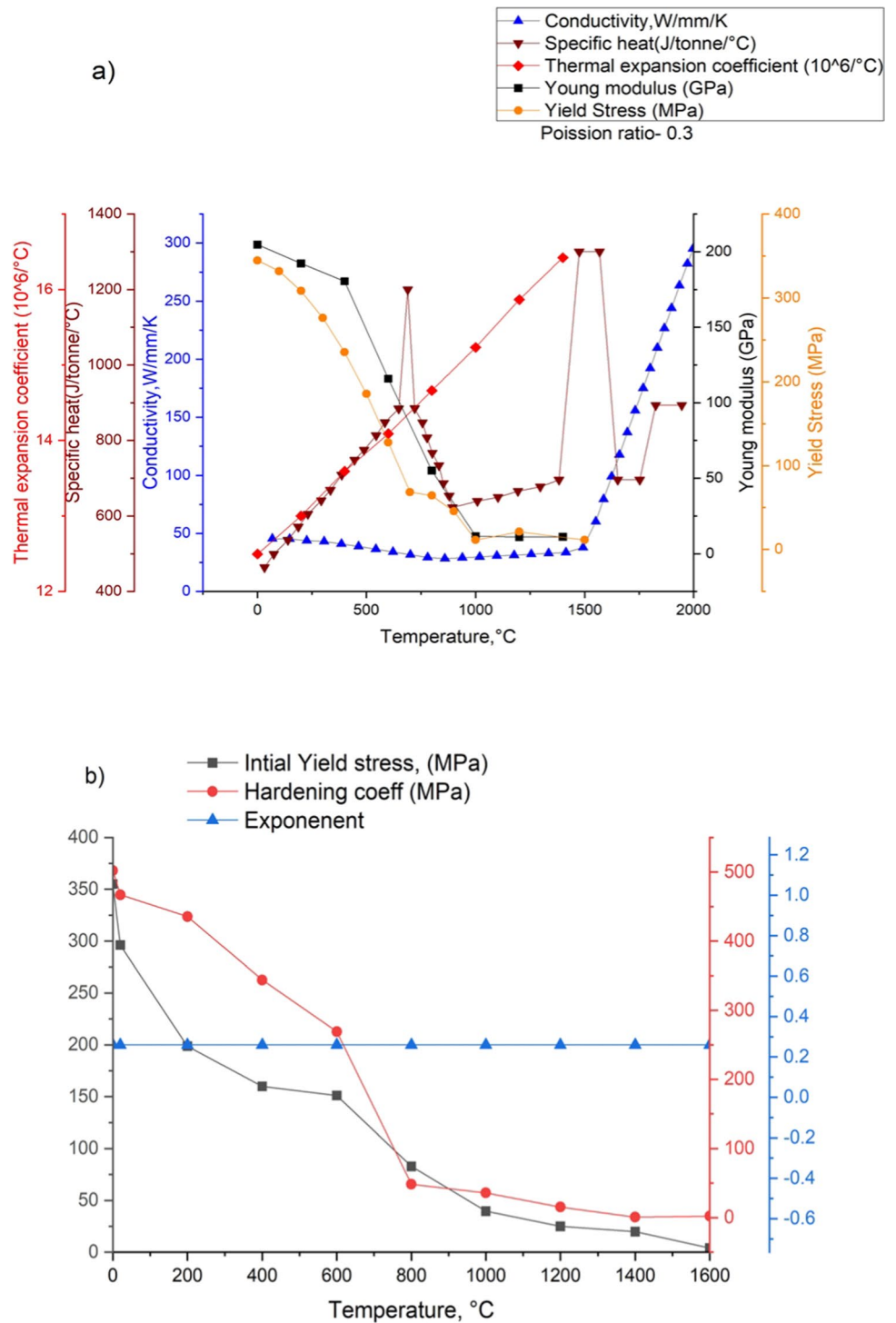


Fig. 3 S355 material temperature-dependent **a** mechanical and material and **b** hardening properties adopted from Bhatti et al. [24]



and b, respectively. Temperature-dependent mechanical and material properties are considered the same for the base and weld metal as per S355 grade. Thermal conductivity from temperature-dependent material properties [25] was doubled between melting and cut-off temperatures to

take the enhanced convection effects of the molten weld pool into account [8]. The isotropic hardening law and rate-dependent power laws were used in this analysis without considering the effect of phase transformations [26] for base and weld materials as shown in Fig. 3b.

2.3.3 Heat source modeling

During thermal analysis, accurate estimation of linear heat input (Q) in J/mm in welding direction is important by approximating the area of the weld pass (A_{pass}) correctly as shown in Fig. 2. Goldak’s double ellipsoid [27] fusion zone length parameters ($c_r + c_f$) (i.e., rear and front part of the torch) were estimated by using Rosenthal’s moving heat source solution for semi-infinite bodies [28]. Various researchers [9, 18, 29–33] have used a simplified model of heat flow analysis for estimating heat input in 2D or axisymmetric numerical models for residual stress estimations. Hold time t_{hold} determination can be estimated by deposited weld at a specified melting temperature according to Eq. (1). Determination of hold time and heat input to avoid overheating in the numerical model was performed by calculating weld pass area (A_{pass}) by using macrographs from WPQR, which we qualified in a previous study [4].

$$t_{hold} = \frac{c_r + c_f}{v} \tag{1}$$

Linear heat approximation for each weld pass was performed analytically to estimate the torch length parameters and hold time as shown in Table 2. A detailed explanation for linear heat input estimation and torch parameters can be found in Bhardwaj and Ratnayake [34]. The Qustom app plugin was used in ABAQUS, which can automatically import the defined geometry and can assign temperature-dependent properties to the relevant sections of the weld and parent metal. This plugin can automatically generate and define weld passes by facilitating easy assignment of the weld bead sequence for each weld pass in multi-pass welds. In the bead assign section of this plugin, hold time can be calculated automatically by inserting analytically derived Goldak’s parameters of the front and rear ($c_r + c_f$) parts of

the torch. Similarly, the weld bead laying sequence and corresponding cooling time can be inserted automatically.

DCAX4: A 4-node linear axisymmetric heat transfer quadrilateral element was used for thermal analysis in ABAQUS. Each weld pass was deposited at a melting temperature of 1500 °C and a cut-off temperature of 1200 °C until it reaches inter-pass from the WPQR. Surface film conditions were provided in the thermal model with a magnitude of $25 \text{ Wm}^{-2} \text{ K}^{-1}$ corresponding to a still air environment for both sides across a thickness and radiation emissivity coefficient of 0.7. After the completion of each pass of the existing weld, sufficient cooling time was provided to the model to reach the ambient temperature conditions seen in Table 2. After its completion, repair weld beads were inserted into the model at set proximity distances of 5, 10, and 15 mm according to the parameters mentioned in Table 2.

2.3.4 Mechanical model

The mechanical model was generated separately in ABAQUS in an uncoupled thermo-mechanical fashion after nodal temperature estimation was matched with available thermocouple data and macrographs from the available WPQR. In the mechanical model, suitable boundary conditions are provided to avoid rigid body motions and over-constraining of the model. In the mechanical analysis, melting temperature was capped to avoid excessively large thermal strains, and cut-off temperatures were set in material properties as per Fig. 3b to avoid a large accumulation of plastic strains. CAX4: A 4-node bilinear axisymmetric quadrilateral element was used for mechanical analysis in ABAQUS. Boundary conditions were applied to eliminate all rigid body motions by restraint at the axial end of the pipe without affecting the stress solution.

Table 2 Hold time and torch parameters for existing and repair welds

Weld pass	v Travel speed (mm/s)	Q (J/mm)	Area of the bead (A_{pass} (mm ²))	C_r Rear length of torch (mm)	C_f Front length of torch (mm)	t_{hold} (s)	Cool down time (s)
Existing weld							
Root	1	913.9	21.99	1.91	0.67	2.58	1800
Hot pass	1.47	988.2	22.29	3.12	0.94	2.77	600
Fill	3.22	746.7	26.01	5.36	1.61	2.17	600
Cap	2.92	894.4	21.4	5.81	1.75	2.69	3600
Repair weld							
Root	1.52	736.0	28	0.70	2.34	2.00	900
Hot pass	5.9	650.3	20.93	2.47	8.23	1.81	600
Fill	5.48	640.6	27.69	2.47	8.22	1.95	600
Cap	4.28	794.2	30.13	2.30	7.66	2.33	3600

3 Results and discussion

The results of hoop and axial residual stress measured from XRD techniques were compared with FEM results for pipe outer and inner surfaces as shown in Figs. 4 and

5, respectively. The measurements were performed on the pipe’s outer surface starting from the left side of the repair weld toe (WT-R) to the right toe of the existing weld (WT-E) and on the pipe’s inner surfaces, i.e., between the repair and existing weld root toes for all proximity distances as

Fig. 4 FEM vs XRD comparison of normalized residual stresses on pipe **a** hoop—outside and **b** hoop—inside for all proximity distances starting from the repair to the existing weld

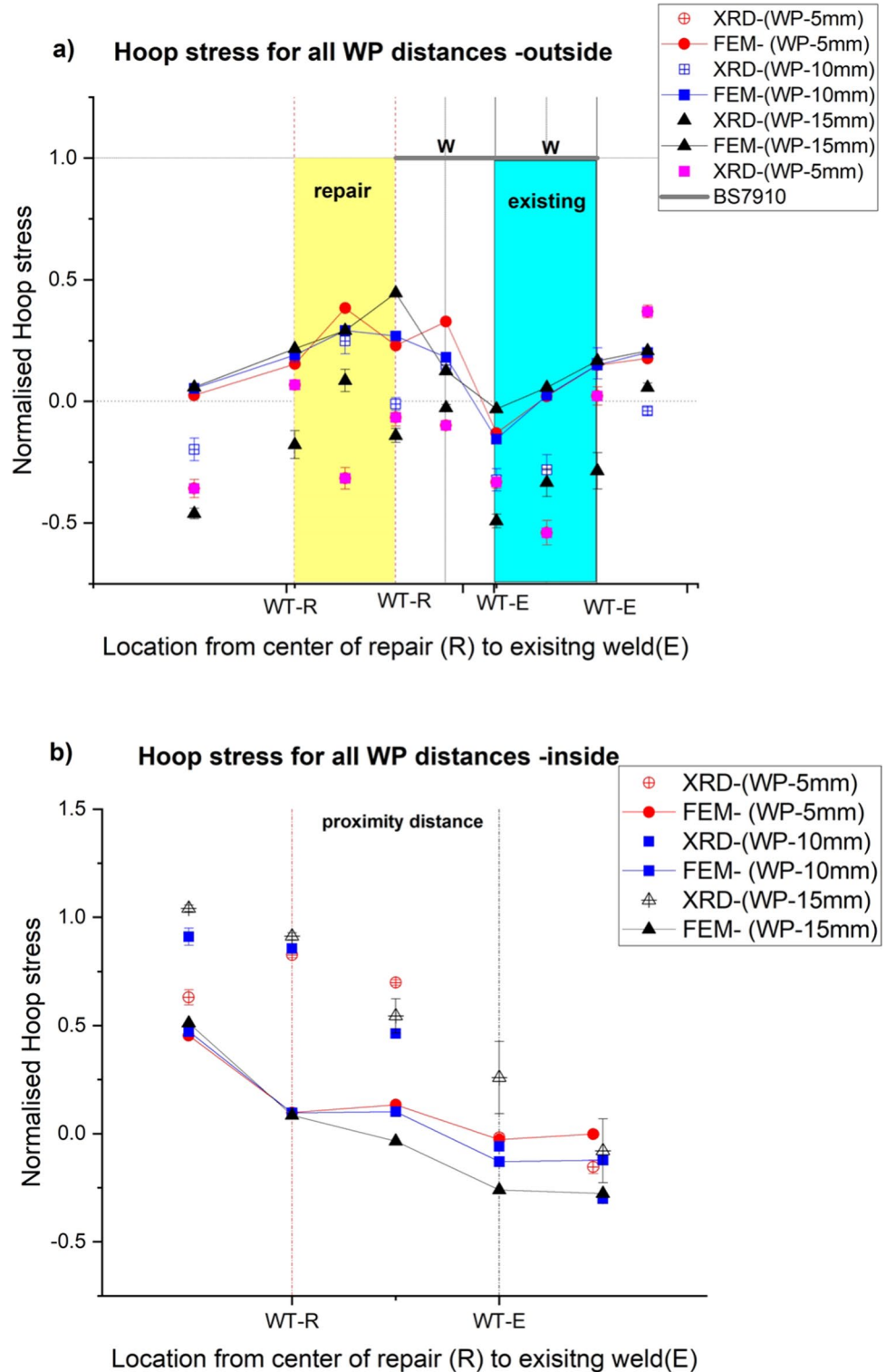
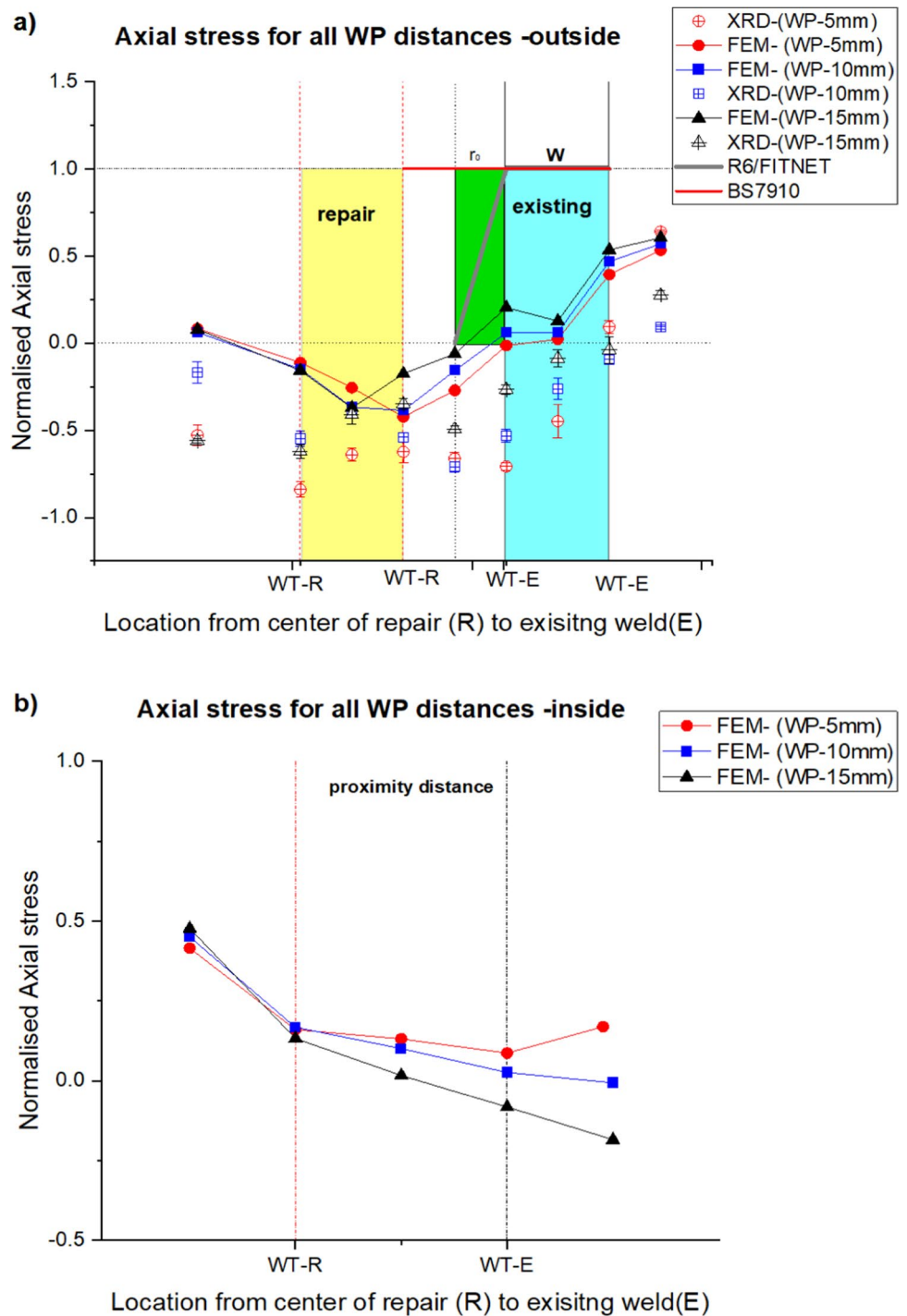


Fig. 5 FEM vs XRD comparison of normalized residual stresses on pipe **a** axial-outside and **b** axial-inside surface (FEM only) for all proximity distances starting from the repair to the existing weld

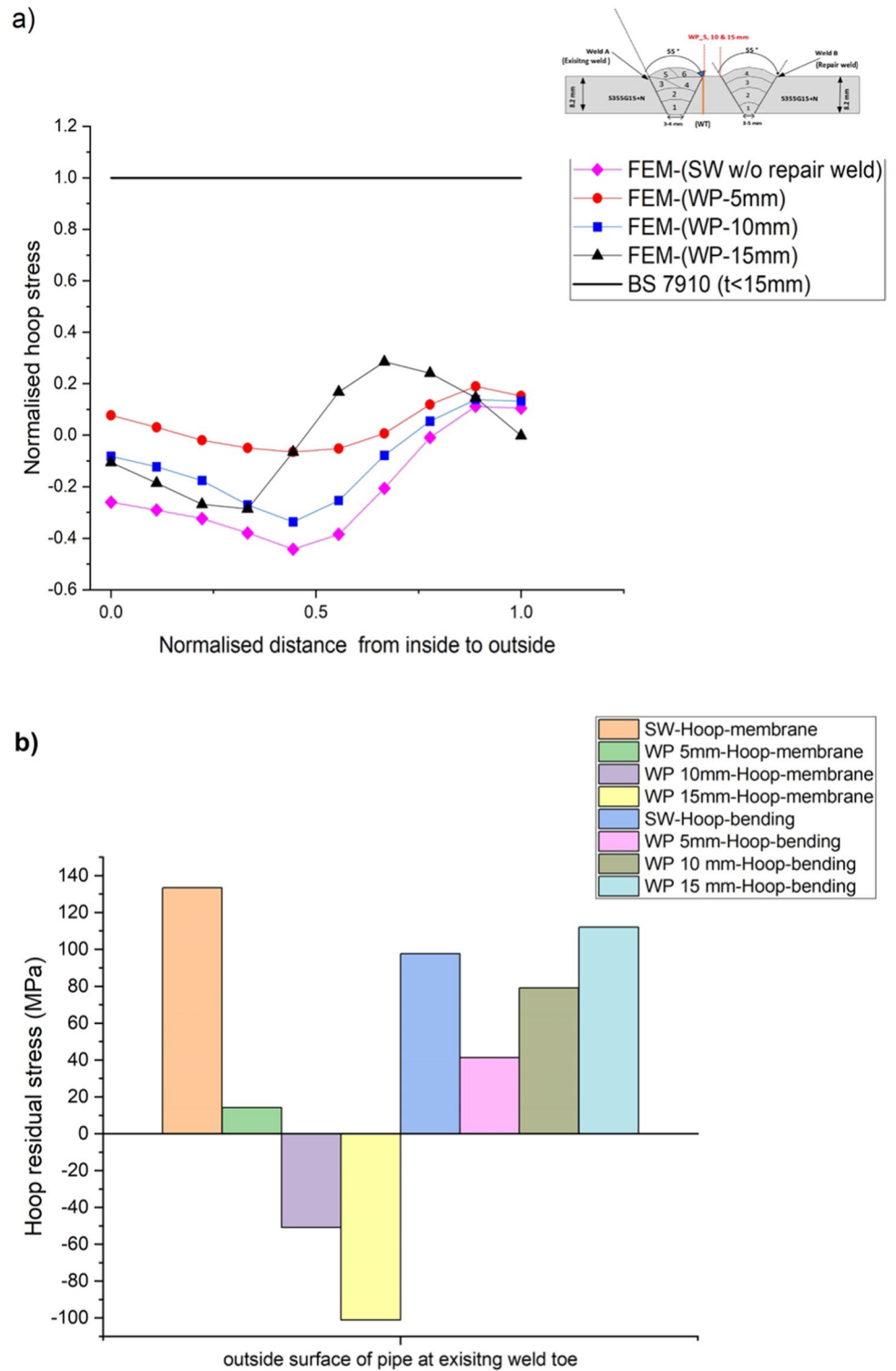


previously shown in Fig. 2. Through-thickness stress distribution at existing weld toe location is also presented in Figs. 6 and 7 for hoop and axial stress components, respectively, for all proximity distances.

3.1 Hoop residual stress: circumferential to weld direction

As shown in Fig. 4a and b, hoop residual stresses were presented for all WP distances starting from the repair weld

Fig. 6 Hoop stress distribution **a** through thickness at existing weld toe location **b** hoop stress linearized components from FEM for all proximity distances

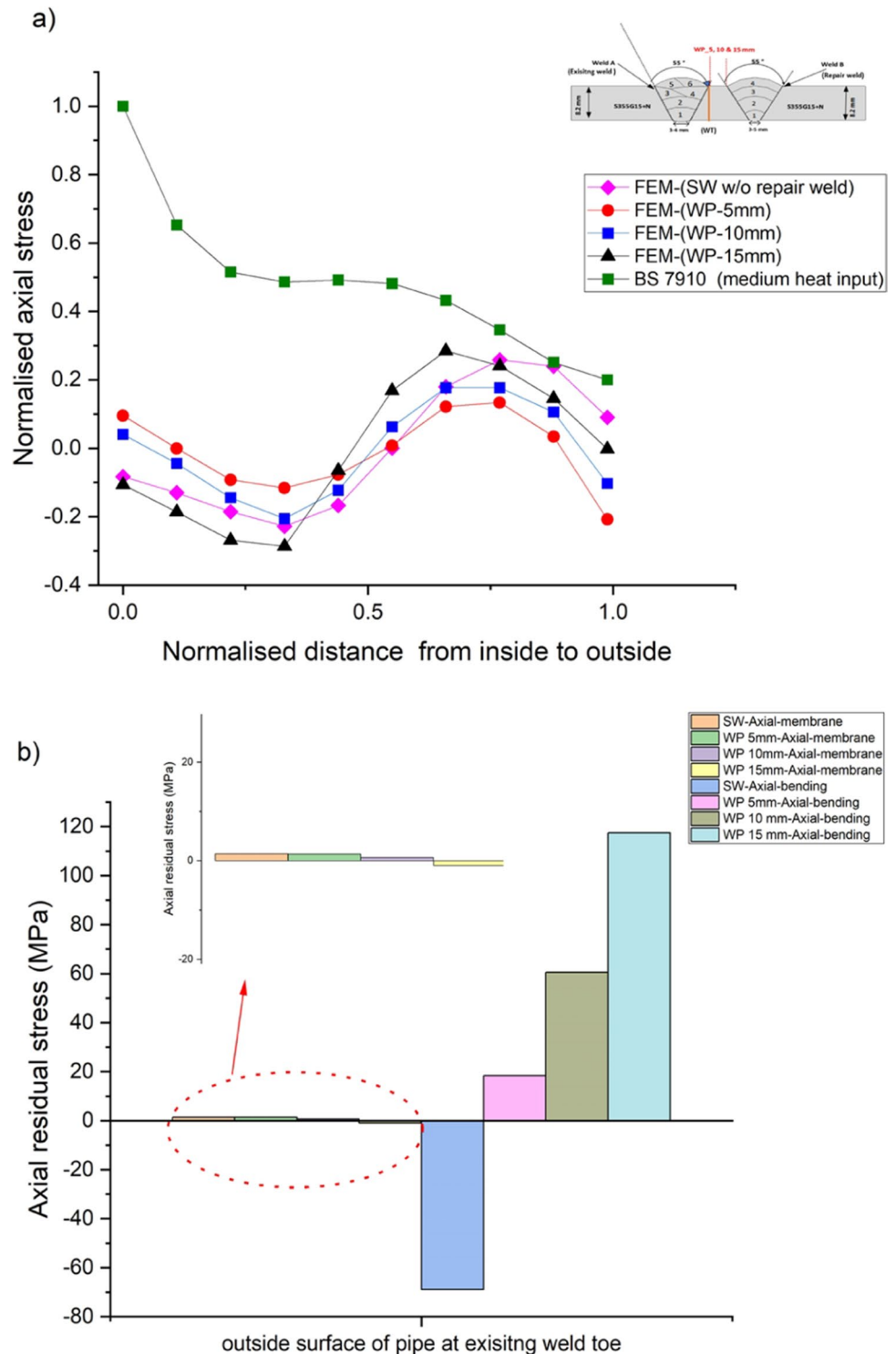


towards the existing weld for the pipe’s outer and inner surfaces, respectively. The figures show that hoop stresses at outer surface proximity regions are mainly compressive in nature. However, pipe inner surface stresses are mainly tensile in nature, starting from the weld toe WT-R (repair) to the WT-E (existing) weld.

3.1.1 Stress measured on the outside of the pipe

The XRD-measured points on the outside surface of the proximity region for 5 and 15 mm WP distances were found to be mainly compressive in nature, whereas 10 mm WPs were found to be on the tensile side as shown in Fig. 4a. The

Fig. 7 Axial stress distribution **a** through thickness at existing weld toe locations **b** axial stress linearized components from FEM for all proximity distances



magnitude for 5 and 15 mm WP samples were found to be negative 20% of the yield strength of S355 material used in this study, whereas 10 mm WP was found to be positive 10% of yield strength. FEM results for 5, 10, and 15 mm WPs showed the same decreasing trend between repair and existing welds, but their magnitude is overpredicted in contrast

to XRD results. It is worth mentioning here that stresses estimated by FEM were overpredicted as the model used in this study does not consider the effect of phase transformations and temperature-dependent properties of filler wires of weld metal. Changes in the final developed profile at proximity regions (i.e., between adjacent welds) can be

attributed to the additional restraint of the repair weld (i.e., due to an additional shrinkage effect) and tempering effect with decreasing distances between their weld toes as seen from the FEM results.

Hoop stresses measured at weld center locations on pipe outer surfaces of repair welds are found to be tensile in nature due to natural restraint in pipe geometries. Generally, hoop stresses are found to be equal to the yield magnitude at weld center locations and are balanced by compressive stresses on adjacent sides of the weld [35, 36]. Due to the sequence of repair welds being welded after the completion of existing welds, stresses found at weld centers of existing welds were found to be normalized or generally compressive in nature. A shrinkage zone-controlled plastic zone leads to the development of yield-level hoop residual stresses around weld toe regions as demonstrated by previous research [29–31, 34] and found to be conservative when compared with fitness for service codes (FFS), e.g., BS 7910 profiles at a distance away from weld toe where W is the width of weld [13]. Due to the use of two different welding processes in simulating the conditions of repair and existing welds with varying heat inputs and sequences of welding, stresses developed at these regions are further normalized. Due to changes in the morphology of the final microstructure developed at proximity regions, as observed in WPQR of proximity welds micrographs, the development of stress at an inter or intra-granular level can be considered the main reason for changes in the final observed residual stress state.

3.1.2 Stress measured inside the pipe

Hoop stresses measured between two WT-R and WT-E locations on the pipe's inner surface by the XRD technique are presented in Fig. 4b. Repair welds exhibited tensile residual stresses equal to or greater than the yield strength of the material, i.e., S355 at WT-R locations, whereas these stresses were found to be converging towards compressive regions at WT-E locations. Stresses developed at proximity regions on pipes' inner surfaces for 5 mm WP from the XRD results were found to be of maximum magnitude, i.e., around 50% yield stress of S355 steel used in this study, which can be attributed to the maximum restraint effect. FEM validation shows a fair agreement with the experimental results; however, the predicted stresses were underpredicted by 25%.

Stresses measured from XRD at WT-E root locations for 5 mm WP distances are minimum at the weld root location due to the maximum compression effect of subsequent passes in a multi-pass weld, as observed by other researchers [35]. This high hoop tensile residual stress that developed at weld root toe locations can be deleterious to the structural integrity of piping, which are subjected to corrosive transport of fluid,

creating a perfect environment for SCC cracking. Stresses measured at proximity regions for 5 mm WP show a global bending behavior, i.e., compression on the outside and tension on the inside, as observed by previous researchers [8] for failures in power piping girth welds [37, 38]. Due to the multiaxial nature of residual stress developed at proximity regions, minimum distance criteria need to be standardized for non-stress-relieved welds to avoid the risk of SCC and reheat cracking.

3.1.3 Through-thickness stress distribution: existing weld vs repair weld

Figure 6a presents the through-thickness hoop stress distribution at the WT location of existing welds for all proximity distances. These FEM-based results are compared with the existing single weld (SW) stress state distribution without the presence of repair welds at proximity. It can be observed that the original state of existing welds follows a tensile distribution on the outer surface and compression on the inner surface of the pipe. For 10 and 15 mm WP distances, hoop stress distribution exhibits almost the same trend with some changes due to the effect of decreasing proximities. For 5 mm WP, due to the maximum effect of restraint and an additional shrinkage effect, hoop stress distribution is changed, and tensile stresses are estimated at pipe outer and inner surfaces at existing weld toes. These profiles also show the overestimation of hoop residual stress in FFS codes like BS 7910 in through-thickness components.

Stress linearized components based on the length scale-based characterization technique [39] and derived from stress decomposition theory are important from a structural integrity perspective. The decomposed components of the membrane and bending are beneficial in determining the fracture driving force in terms of stress intensity factor (K). Membrane components provide maximum contributions in crack driving force followed by bending as demonstrated by various researchers in the past [3, 9, 39]. Figure 6b presents the decomposed component of membrane and bending for hoop stress for all WP distances at existing weld toe locations at pipe outer surfaces. It can be observed that the hoop-membrane component is the maximum for 5 mm WP in contrast to 10 and 15 mm WP in contrast to SW stress state, which was found to be the maximum. Higher membrane hoop stress exerts the maximum circumferential shrinkage force which can be deleterious to pressure-containing pipes as additional hoop component is developed in addition to natural hoop restraint in pipe girth welds. The hoop-bending component was found to be the maximum for the 15 mm WP distance and found to be comparable with existing SW original state, which implies increased radial restraint.

3.2 Axial residual stress: perpendicular to weld direction

As shown in Fig. 5a and b, axial residual stress distribution is presented for all WP distances starting from the repair weld towards the existing weld on pipe outer and inner surfaces. It can be observed that axial stresses change from compressive to tensile and vice versa starting from the repair to the existing weld on pipes' outer and inner surfaces, respectively.

3.2.1 Stress measured on the outside of pipes

WRS measured by the XRD technique for all WP distances were found to be compressive at the weld center location of repair welds and shift towards tensile regions at existing weld center locations as shown in Fig. 5a. Stresses measured at the proximity region were found to be compressive from the XRD technique for all proximity distances and found between negative 50% and 70% magnitude of the yield stress for the S355 material. FEM results were estimated to be in reasonable agreement, except for weld center locations. This can be attributed to the use of S355 temperature-dependent mechanical properties for weld metal locations of repair and existing welds in FEM models.

Axial stress distribution is primarily affected by the mismatch in axial strains and due to different expansion and contraction properties of filler wires used in the fabrication of repair and existing welds. This mismatch is compensated by plastic straining of repair welds and proximity regions when compared with elastic deformation of the parent metal as noticed by Bouchard [37] while studying the overlapping repair weld length effect on the existing weld. Song and Dong [8] made a similar observation while deciding repair length optimum size, i.e., maximum possible length, but width should be as narrow as possible, and its depth as shallow as possible. Axial residual stress profiles at a distance away from weld in FFS codes were found to match close to the yield boundary zone defined in R6 code [12] at distance away from weld in contrast to BS 7910 [13].

3.2.2 Stress measured inside the pipe

Axial residual stresses estimated at pipe inner surfaces from the FEM study were found to be tensile at the repair weld root toe location and moving toward a zero-stress state or compression at the existing weld root toe as shown in Fig. 5b. For the 5 mm WP distance, tensile stresses were observed at weld root toe locations of existing welds in contrast to compressive stresses found at 10 and 15 mm WPs. This can be attributed to maximum restraint at WP 5 mm distance and the multiaxial stress state developed at proximity regions. Tensile axial residual stress was also observed at root toe locations of existing and repair welds at 6 mm depth from the top of the weld cap by neutron diffraction

experiments [19]. Axial residual stresses contribution is important for determining crack driving parameters for components subjected to axial loadings; hence, their estimation is important for determining the minimum distance for repair weld placement in piping subjected to corrosive mediums.

3.2.3 Through-thickness stress distribution: existing weld vs repair weld

Figure 7a presents through-thickness axial stress distribution for all proximity distances compared with the existing single weld (SW) stress distribution without the presence of repair welds in proximity. It can be observed that the original state of SW follows a distribution of a self-balancing state with compression on the outer surface balanced by tension at mid thickness followed by compression on the inner surfaces of pipe. The same observation was noticed for 10 and 15 mm WP distances; however, for 5 mm WP, tensile axial stresses were estimated at weld root toe locations of existing weld toe locations. Tensile 10% and 20% compression S355 yield was estimated by FEM at pipes' inner and outer surfaces, respectively, for 5 mm WP. Twenty percent compression can be attributed to maximum tempering and interaction taking place between weld toe of repairs and existing welds in contrast to 10 and 15 mm WP. At pipe inner surfaces, tensile stresses were observed in contrast to 10 and 15 mm WP due to the maximum effect of restraint and multi-axial stress developed at proximity regions.

The membrane component in the axial direction was found to be negligible [15, 30] for different t/t geometries unless final assembly welds have restraints. Stress decomposed factors of axial residual stress at pipe outer surfaces are presented in Fig. 7b where the membrane component for 5 mm WP was found to be higher than 10 and 15 mm WP and comparable with the SW axial component. The bending component was found highest for 15 mm WP in contrast to 5 and 10 mm WP. Macrographs of 15 mm WP generated from WPQR in a previous study [4] displayed maximum distortion in axial or transverse directions in contrast to 5 and 10 mm WP. This can cause high primary and secondary bending stresses, which are deleterious to pipe welds subjected to axial loading conditions under repeated loading conditions leading to fatigue failures.

4 Conclusion

In this article, numerical and experimental investigations were conducted to estimate welding-induced residual stress between weld toes of repair girth welds placed at set proximity distances to an existing girth weld. XRD measurements were conducted by using a Proto iXRD® compact instrument at SINTEF/NTNU/IMT, Norway, on pipe outer and inner surfaces, respectively. These measurements were validated with a FEM-based

thermo-mechanical model in ABAQUS® and were found to have a fair agreement with the experimental results. This case study was an extension of a previously qualified welding procedure qualification record and residual stress measurement by neutron diffraction between proximity welds on a structural steel S355 grade pipe. Residual stresses were quantified using the stress decomposition technique for determining the through-thickness stress state profile and highlights the contribution of hoop and axial decomposed components of membrane and bending which are useful in estimating stress intensity factors due to residual stress used in crack assessment procedures. The major findings of this study are reported below:

- Residual stress distribution between repairs and existing weld toes on pipes' outer surfaces are strongly influenced by the distance maintained from their weld toe as a maximum tempering effect was noticed in the hoop and axial directions for 5 mm proximity due to the closest interaction of adjacent weld toes.
- The residual stress distribution on pipe inner surfaces between adjacent weld root toes exhibits the development of harmful tensile stress formation at existing weld root toes which can be deleterious to SCC and reheat cracking in aging welds of power and process piping's structures.
- The sequence and restraint of repair weld fabrication in proximity to existing welds were identified as major factors in determining the final residual stress development of tension at existing weld toe locations at pipe outer and inner surfaces by using the XRD technique.
- FEM models were found to have a reasonably fair agreement with measured XRD results. Variations in results can be attributed to a lack of temperature-dependent mechanical properties for filler metals, type of hardening model, and the exclusion of phase transformations in FEM models.
- Linear 2D heat input approximation and Rosenthal's moving heat source solution for avoiding overheating problems and estimating Goldak's torch parameter, respectively, in thermal models, from weld macrographs have proven to be an effective technique for estimating residual stresses in FEM.
- An increase in the decomposed component of membrane stress by stress decomposition theory in the hoop and axial directions for the closest proximity distance was identified as an important technique for identifying important parameters for determining fracture driving forces used in structural integrity procedures for cracks in welds.
- In deciding minimum distance criteria for the placement of repair welds in proximity to existing welds, residual stress profile estimation at distances where they completely vanish from weld toe locations needs to be recommended based on repair weld geometry, i.e., radius to thickness ratio, heat input of the repair welding process, and the sequence of welding leading to additional restraints.

Further validation with a FEM-based numerical model considering the effect of metallurgical and phase transformations needs to be developed during the defect assessment procedures of welds.

Acknowledgements We would like to acknowledge the support of SINTEF Ocean/Structural Engineering and NTNU/IMT, Norway, for providing free access to the Proto iXRD instrument for measuring residual stresses. We would also like to acknowledge the support of Qustom apps, USA, for providing free access to their plugin that we used for modeling welds in ABAQUS.

Author contribution Sachin Bhardwaj: conceptualization, experimentation, investigation, methodology, visualization, writing—original draft, writing—review and editing, and data analysis. Sigmund Kyrre Aas: experimentation, investigation, analysis, and writing—review and editing. R.M. Chandima Ratnayake: conceptualization, formal analysis, review and editing, funding acquisition, project administration, and supervision.

Funding Open access funding provided by University of Stavanger & Stavanger University Hospital The research was fully funded by the Norwegian Ministry of Education (Internal PhD project No. IN-12168). This work was carried out as part of a PhD research project, performed at the University of Stavanger, Norway.

Data availability All data generated and analyzed during this research are included in this published article.

Code availability Not applicable.

Declarations

Ethics approval Not applicable.

Consent to participate Not applicable.

Consent for publication Not applicable.

Conflict of interest The authors declare no competing interests.

Open Access This article is licensed under a Creative Commons Attribution 4.0 International License, which permits use, sharing, adaptation, distribution and reproduction in any medium or format, as long as you give appropriate credit to the original author(s) and the source, provide a link to the Creative Commons licence, and indicate if changes were made. The images or other third party material in this article are included in the article's Creative Commons licence, unless indicated otherwise in a credit line to the material. If material is not included in the article's Creative Commons licence and your intended use is not permitted by statutory regulation or exceeds the permitted use, you will need to obtain permission directly from the copyright holder. To view a copy of this licence, visit <http://creativecommons.org/licenses/by/4.0/>.

References

1. Antaki GA (2003) Piping and pipeline engineering: design, construction, maintenance, integrity, and repair. Marcel Dekker, New York
2. Lotsberg I (2016) Fatigue design of marine structures. Cambridge University Press, Cambridge
3. Song S, Dong P (2014) Residual stresses in weld repairs and mitigation by design. In: ASME 2014 33rd International Conference on Ocean, Offshore and Arctic Engineering

4. Bhardwaj S, Ratnayake RMC (2022) Welding Procedure Qualification Record (WPQR) for welds fabricated at proximity. *Int J Adv Manuf Technol*
5. Bhardwaj S, Ratnayake RMC (2020) Challenges due to welds fabricated at a close proximity on offshore structures, pipelines, and piping: State of the art. In: ASME 2020 39th International Conference on Ocean, Offshore and Arctic Engineering
6. Institute AP (2015) API 2200 Repairing Hazardous Liquid Pipelines. API, USA
7. DNVGL, DNV-OS-F101 (2013) In: Submarine Pipeline Systems. DNV, Norway
8. Song S, Dong P (2017) Residual stresses at weld repairs and effects of repair geometry. *Sci Technol Weld Join* 22(4):265–277
9. Dong P (2018) On repair weld residual stresses and significance to structural integrity. *Weld World* 62(2):351–362
10. Dong P, Zhang J, Bouchard PJ (2001) Effects of repair weld length on residual stress distribution. *J Press Vessel Technol* 124(1):74–80
11. American Petroleum Institute, API (2007) RP 579-1/ASME FFS-1. American Petroleum Institute, Houston
12. British Energy Generation Ltd (2013) Procedure R6 Revision 4, assessment of the integrity of structures containing defects
13. British Standard, BS (2019) 7910 Guide to methods for assessing the acceptability of flaws in metallic structures. UK
14. Dong P et al (2014) On residual stress prescriptions for fitness for service assessment of pipe girth welds. *Int J Press Vessels Pip* 123(124):19–29
15. Bhardwaj S, Ratnayake RMC (2020) Residual stress estimation in defect assessment procedures at weld toe and away locations on girth welds: Review of key parameters. *Theor Appl Fract Mech* 102848
16. Acevedo C, Nussbaumer A (2013) Effect of tensile residual stresses on fatigue crack growth and S-N curves in tubular joint in compression. *Int J Fatigue* 36:171–180
17. Larsson M et al (2021) Experimental residual stress investigation of weld joints fabricated at a close proximity in S420 structural steel 357–376
18. Brickstad B, Josefson BL (1998) A parametric study of residual stresses in multi-pass butt-welded stainless steel pipes. *Int J Pressure Vessels Pip* 75(1):11–25
19. Bhardwaj S et al (2022) Experimental investigation of residual stress distribution on girth welds fabricated at proximity using neutron diffraction technique. *Int J Adv Manuf Technol* 121(5):3703–3715
20. Hauk V (1997) 2 - X-ray diffraction. *Structural and Residual Stress Analysis by Nondestructive Methods*. In: Hauk V (ed) Elsevier Science, Amsterdam, pp 17–65
21. ABAQUS (2020) User's manual Version 7
22. Qustomapps (2019) Qustom weld plug in ABAQUS
23. Yaghi A, Becker AA (2005) State of the art review - weld simulation using finite element methods. NAFEMS2005, Glasgow
24. Bhatti AA et al (2015) Influence of thermo-mechanical material properties of different steel grades on welding residual stresses and angular distortion. *Mat Des* (1980–2015) 65:878–889
25. Barsoum Z, Lundbäck A (2009) Simplified FE welding simulation of fillet welds – 3D effects on the formation residual stresses. *Eng Fail Anal* 16(7):2281–2289
26. Zhu J, Khurshid M, Barsoum Z (2019) Accuracy of computational welding mechanics methods for estimation of angular distortion and residual stresses. *Weld World* 63(5):1391–1405
27. Goldak JA, Akhlaghi M (2005) *Computational Welding Mechanics*. Comput Weld Mech 1–321
28. Rosenthal D (1946) The theory of moving sources of heat and its application to metal treatments. ASME, Cambridge
29. Pei X, Song S, Dong P (2015) An analytical method for estimating welding-induced plastic zone size for residual stress profile development. In: ASME 2015 Pressure Vessels and Piping Conference
30. Song S, Dong P, Pei X (2015) A full-field residual stress estimation scheme for fitness-for-service assessment of pipe girth welds: Part I - Identification of key parameters. *Int J Press Vessels Pip* 126–127:58–70
31. Song S, Pei X, Dong P (2015) An analytical interpretation of welding linear heat input for 2D residual stress models. In: ASME 2015 pressure vessels and piping conference
32. Yaghi A et al (2010) A comparison between measured and modeled residual stresses in a circumferentially butt-welded P91 steel pipe. *J Press Vessel Technol* 132
33. Bhardwaj S, Ratnayake RMC (2021) Comparison between shrinkage strain and FEM thermo-mechanical method for estimation of welding induced residual stresses. In: ASME 2021 40th International Conference on Ocean, Offshore and Arctic Engineering
34. Bhardwaj S, Ratnayake RMC (2021) Estimation of welding-induced plastic zone size and residual stress levels: Linear Heat Input Approximation. In: ASME 2021 40th International Conference on Ocean, Offshore and Arctic Engineering
35. Alipooramirabad H et al (2015) Quantification of residual stresses in multi-pass welds using neutron diffraction. *J Mater Process Technol* 226:40–49
36. Stacey A et al (2000) Incorporation of residual stresses into the SIN-TAP defect assessment procedure. *Eng Fract Mech* 67:573–611
37. Bouchard PJ et al (2005) Measurement of the residual stresses in a stainless steel pipe girth weld containing long and short repairs. *Int J Press Vessels Pip* 82(4):299–310
38. Gandy D, Findlan S, Viswanathan R (2001) Weld Repair of Steam Turbine Casings and Piping—An Industry Survey. *J Press Vessel Technol* 123
39. Dong P (2008) Length scale of secondary stresses in fracture and fatigue. *Int J Press Vessels Pip* 85:128–143

Publisher's note Springer Nature remains neutral with regard to jurisdictional claims in published maps and institutional affiliations.